CAU-Net: A Convolutional Attention U-Network For Radar Signal Deinterleaving

Yejian Zhou, Ye Zheng, Shaopeng Wei, Lei Zhang, and Zhenyu Wen, *Senior Member, IEEE*

***Abstract*— The deinterleaving of radar signals is designed to segregate distinct pulses within a composite signal, facilitating the detailed analysis of individual components. This process is pivotal in situational awareness applications, including target signal interception and cognitive jamming antagonism. In the existing electromagnetic environment, the radar emitter pulse modulation parameters will be jitter modulated to improve its anti-identification ability, leading to the lack of integrity of the pulse features obtained from the measurements and the degradation of the deinterleaving performance of the existing methods. In this letter, a Convolutional Attention U-Network (CAU-Net) is proposed to deinterleave the original signal. Guided by the attentional mechanism, the feature of the original signal is extracted by the Attention Down-Sampling (ADS) block without necessitating pulse measurement. Then, it is used to classify the predicted pulses by the Feature Fusion Up-Sampling (FFUS) block, with the prior maximum number of radar emitters in each sample. The experimental results demonstrate the superior performance of the proposed CAU-Net in terms of deinterleaving and complexity, and its robustness is confirmed under various noise conditions.**

***Index Terms*— Radar signal deinterleaving, deep convolutional network, convolutional attention mechanism, parameter estimation.**

I. Introduction

RADAR signal deinterleaving serves to segregate distinct pulses from a high-density mixed pulse stream in multi-emitter scenarios. This process provides essential support for emitter identification, target tracking, and subsequent decision-making, making it a key component of Electronic Support Measurement (ESM) systems.

In conventional works on radar signal deinterleaving, pulse streams are described using Pulse Descriptive Words (PDWs), such as Direction Of Arrival (DOA) and Pulse Width (PW). The deinterleaving process is often accomplished through parameter matching. For example, Saperstein proposed the template matching approach, wherein deinterleaving is achieved by constructing a radar pulse database and comparing it with the received signal [1]. After that, other periodic features of pulse streams are introduced in the relative works, including Cumulative Difference Histogram (CDIF) [2] and Sequential Difference Histogram (SDIF) [3]. To address the effect of subharmonics on this sort of method, the Pulse Repeat Interval (PRI) transform is proposed [4]. It achieves the parameter estimation by utilizing a complex-valued integral during the histogram calculation.

With the advancement of deep learning techniques, several exploratory methods utilizing neural networks have been proposed in recent years [5], [6], [7], [8], [9], [10], [11], [12], [13]. A three-layer neural network is designed to facilitate the categorization of PRI modulation based on the statistics feature of the time-domain signal [5]. In [7], Recurrent Neural Network (RNN) is employed to extract the sequential feature in pulse streams for the deinterleaving task. With the attention mechanism, the classification of pulse streams is achieved by the Gated Recurrent Unit (GRU) [8]. Chao et al. integrated the concept of semantic segmentation into radar deinterleaving, employing Bidirectional Recurrent Neural Networks (BRNN) to achieve radar pulse deinterleaving [10]. In all, these methods rely on the sufficient PWDs of each pulse to achieve the deinterleaving, which hardly can be ensured during the measurement processing. It directly affects the deinterleaving performance. In addition, these methods require the knowledge of the number of radar emitters in the pulse before the identification process.

This letter presents a novel approach to deinterleaving employing a CAU-Net framework. This technique stands out by utilizing the original received signal directly for deinterleaving, thus obviating the necessity for additional preprocessing steps. We extract multiscale features of pulse spatial location information from the received signal through the ADS block. Subsequently, the extracted multiscale features undergo continuous fusion and deconvolution via the FFUS block to yield the prediction results. Notably, this algorithm surpasses the constraints of existing radar signal deinterleaving methods grounded in deep learning, which typically demand prior knowledge (e.g., the number of radar emitters). Furthermore, it achieves precise de-interleaving even amidst fluctuations in the number of radar emitters.

The main contributions of this article are as follows:

- The proposed method CAU-Net does not require PDWs and uses the original signal as a deinterleaving object. In this way, problems such as measurement errors,

Manuscript received 10 April 2024; revised 8 May 2024; accepted 21 May 2024. Date of publication 24 May 2024; date of current version 12 July 2024. This work was supported in part by the Zhejiang Provincial Natural Science Foundation of China (Grant LY23F010012), and in part by the National Natural Sciences Foundation of China (Grants 62101494 and 62301612). The associate editor coordinating the review of this letter and approving it for publication was G. Interdonato. *(Corresponding author: Zhenyu Wen.)*

Yejian Zhou is with the College of Information Engineering, Zhejiang University of Technology, Hangzhou 310023, China, and also with the School of Computer Science and Engineering, Nanjing University of Science and Technology, Nanjing 210094, China (e-mail: zhouyejian25@163.com).

Ye Zheng and Zhenyu Wen are with the College of Information Engineering, Zhejiang University of Technology, Hangzhou 310023, China (e-mail: 211122030099@zjut.edu.cn; zhenyuwen@zjut.edu.cn).

Shaopeng Wei is with the College of Oceanography and Space Informatics, China University of Petroleum (East China), Qingdao 266580, China (e-mail: spwei@upc.edu.cn).

Lei Zhang is with the School of Electronics and Communication Engineering, Sun Yat-sen University (Shenzhen Campus), Shenzhen 518107, China (e-mail: zhanglei57@mail.sysu.edu.cn).

Digital Object Identifier 10.1109/LCOMM.2024.3404957

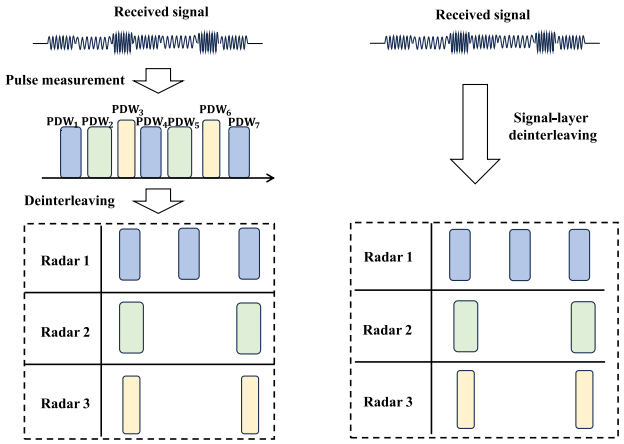

Fig. 1. The processing comparison between the PDWs-based method and proposed method. (Left: the PDWs-based method; Right: the proposed signal-layer deinterleaving method.

pulse loss, and spurious pluses during the pulse measurement are avoided, and the robustness of the deinterleaving process is enhanced.

- To the best of out knowledge, it is first time that a deinterleaving network has been proposed to solve the problem of identifying multiple emitters. The proposed CAU-Net architecture enhances the ability of the model to flexibly adapt to samples with varying numbers of radar emitters by CBAM, improving the broad applicability of deep learning methods in the field of radar deinterleaving.

II. Problem Description

The conventional method based on PDWs encounters challenges in precisely deinterleaving radar emitters exhibiting similar signal types and intricate signal modulation. In order to capitalize on the characteristics of the original signal, this letter explores a deinterleaving approach grounded in received signals, termed signal-layer deinterleaving, as depicted in Fig.1.

The Linear Frequency Modulation (LFM) signal stands out as one of the frequently employed signals in modern radars, featuring a substantial time-bandwidth product. This characteristic allows for the simultaneous attainment of an extended range and distance resolutions. Consequently, this signal type is chosen as the transmit waveform, and its time-domain signal expression is articulated as follows [14]:

$$s\left(t\right)=A\cdot rect\left(\frac{t}{T_p}\right)\exp\left[j2\pi\left(f_0t+\frac{1}{2}kt^2\right)\right] \tag{1}$$

where A is the signal amplitude, T_p is the time width, f_0 is the center frequency, $k=B/T_p$ is frequency modulation slope, and B is the bandwidth. The rectangular function is defined as follows:

$$rect\left(\frac{t}{T_p}\right)=\begin{cases}1, -\frac{T_p}{2}\le t\le\frac{T_p}{2}\\ 0, otherwise\end{cases} \tag{2}$$

The modulation mode of a signal significantly influences the performance and functionality of a radar. Traditional methods identify constant modulation and staggered modulation, both of which exhibit limited anti-interference capabilities. This letter introduces and employs the PRI Jittered modulation and PW Jittered modulation modes in simulation experiments. The jittered PRI sequence fluctuates around a specific PRI value, with the jitter range consistently varying between 1% and 30% of the PRI value. The jittered values are random, typically following a Gaussian or uniform distribution [6]. In subsequent experiments, the uniform variation has been employed, and the values of the jittered PW sequence align with the previously mentioned description.

$$T_r'=\left(1-\alpha+2\alpha\cdot rand\right)\cdot T_r \tag{3}$$

$$T_p'=\left(1-\alpha+2\alpha\cdot rand\right)\cdot T_p \tag{4}$$

where T_r' is the value of PRI, T_r is the constant PRI, T_p' is the value of PW, T_p is the constant PW, α is jittered rate.

Assuming that there are N radar emitters, the n-th radar emitter a total of M pulses are emitted during a Coherent Processing Interval (CPI), the first pulse time of arrival $\mathrm{TOA_{n,0}}$ and the start time of the m-th pulse is $t_{n,m}$. According to Eqs (1)-(4), the time domain expression of the received signal is as follows:

$$S\left(t\right)=\sum_{n=1}^{N}\sum_{m=1}^{M}A_n\cdot rect\left(\frac{t-t_{n,m}}{T_p'}\right)\exp\left(j\pi k(t-t_{n,m})^2\right) \tag{5}$$

$$t_{n,m}=\begin{cases}\mathrm{TOA_{n,0}}, m=1\\ \mathrm{TOA_{n,0}}+\sum_{i=1}^{m-1}T_{r,i}', m\ge 2\end{cases} \tag{6}$$

where f_0 equals to 0 after the down-conversion processing.

Based on the above derivation, PRI, PW, and PA are used as the primary features for distinguishing each radar emitter pulse. To learn these features, we need to train the model using the location of each pulse from each source as ground truth. Unlike image processing, pulses from multiple radar sources can coexist within a time interval, and therefore the sampling points during that time interval have multiple semantic information. To overcome the above problem, we set up N channels with the same length as the length of the signal sequence according to the number of radar emitters, and if the pulse signal of the n-th radar source occurs in a certain period, all the sampling points in the corresponding period of the n-th channel will be of category 1, and the rest of the sampling points will be of category 0. Finally, we supervise the training of the model using the N channel as the labels.

III. The Proposed Method

To deinterleave the original signal when the number of radar emitters is unknown, we propose a CAU-Net to accomplish the deinterleaving task, as shown in Fig.2. In the proposed network, multiscale features are extracted by an attention down-sampling block, and fused to achieve deinterleaving by a feature fusion up-sampling block. Furthermore, it is crucial to align the channels of the last layer of the decoder with the maximum number of radar emitters in the received signal. This alignment ensures that data from all potential numbers of radar emitters can be processed simultaneously. Details are below.

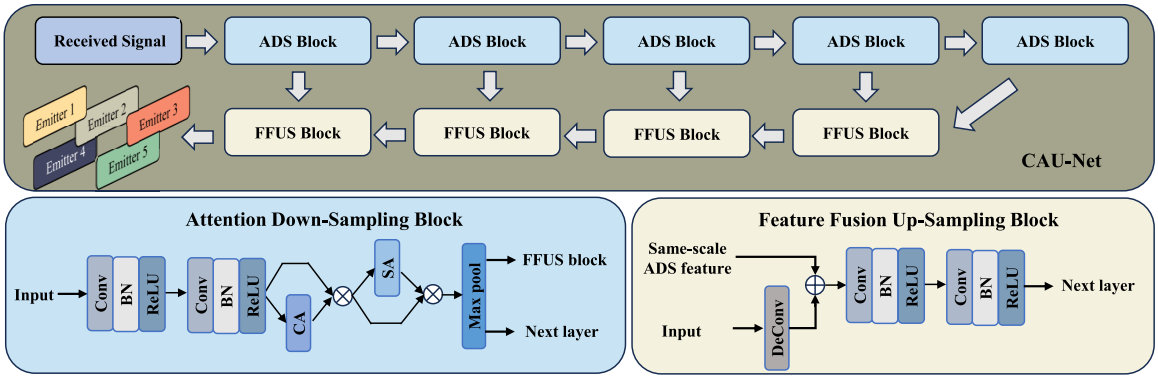

Fig. 2. Overall framework of our proposed model.

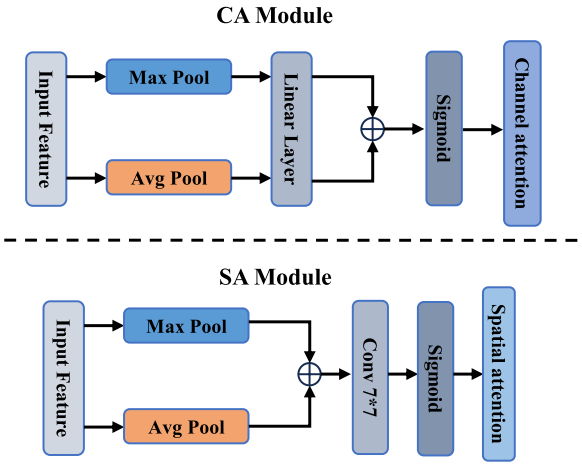

Fig. 3. Diagram of each attention sub-module.

A. Key Modules

The architectures of the ADS block and the FFUS block are depicted in Fig.2. The ADS block consists of one convolutional layer, one batch norm layer, one pooling layer, and one CBAM layer. The convolutional layer has a convolutional kernel size of 3×3, strides of 1, and padding of 1. The batch norm layer maps the input to a standard normal distribution, which facilitates model training. The activation function is the Rectified Linear Unit (ReLU). The pooling layer uses a max-pooling size of 2×2. Each CBAM layer consists of two sequential submodules: the Channel (CA) module and the Spatial (SA) module. The intermediate feature map undergoes adaptive refinement through CBAM in every convolutional block of deep networks. As illustrated in Fig. 3, the CA module employs both max-pooling outputs and average-pooling outputs with a shared network, while the SA module utilizes similar outputs pooled along the channel axis, forwarding them to a convolutional layer. The CA weights W_c and the SA weights W_s are computed by the following equations.

$$W_c(f) = \sigma\left(Linear\left(avgpool\left(f\right)\right) + Linear\left(maxpool\left(f\right)\right)\right) \tag{7}$$

$$W_s(f) = \sigma\left(conv_{7\times7}\left(concat\left(avgpool\left(f\right), maxpool\left(f\right)\right)\right)\right) \tag{8}$$

TABLE I
MAIN PARAMETERS OF SIMULATION SAMPLES

	PW [ms]	PRI [ms]	TOA [ms]	Modulation mode	Jitter rate
Emitter 1	[0.1,0.3]	[2,4]	0	Jittered	0.2
Emitter 2	[0.1,0.3]	[2,4]	0.2	Jittered	0.2
Emitter 3	[0.1,0.3]	[2,4]	0.4	Jittered	0.2
Emitter 4	[0.1,0.3]	[2,4]	0.6	Jittered	0.2
Emitter 5	[0.1,0.3]	[2,4]	0.8	Jittered	0.2

where f is the input feature, σ denotes the sigmoid function, $Linear\left(\cdot\right)$ is linear layer, $concat$ denotes channel concatenation.

The overall attention process can be summarized as follows:

$$f' = W_c\left(f\right) \otimes f$$
$$f'' = W_s\left(f'\right) \otimes f' \tag{9}$$

where $\otimes$ denotes element-wise multiplication.

The FFUS block comprises an up-sampling of the feature map, succeeded by a 2×2 convolution that reduces the number of feature channels by half. This is followed by concatenation with the correspondingly cropped feature map from the encoder and two 3×3 convolutions, each followed by a ReLU.

B. Loss Function

Given the predicted deinterleaving signal $\hat{y}_{l,n}$ and the ground truth $y_{l,n}$, the formula for the prediction loss is calculated below:

$$Loss = \frac{1}{L \cdot N} \sum_{l=1}^{L} \sum_{n=1}^{N} \left(\hat{y}_{l,n} - y_{l,n}\right)^2 \tag{10}$$

where L is the length of the signal sequence, $\hat{y}_{l,n}$ and $y_{l,n}$ represent the probability and the ground truth that the l-th sampling point of the n-th channel is radar emitter signal, respectively.

IV. EXPERIMENTS

A. Design of Experiments

To evaluate the viability of the proposed method, we conducted simulations where the number of emitters in each sample ranged from two to five. The primary parameters for each radar are detailed in Table I. All emitters maintain a

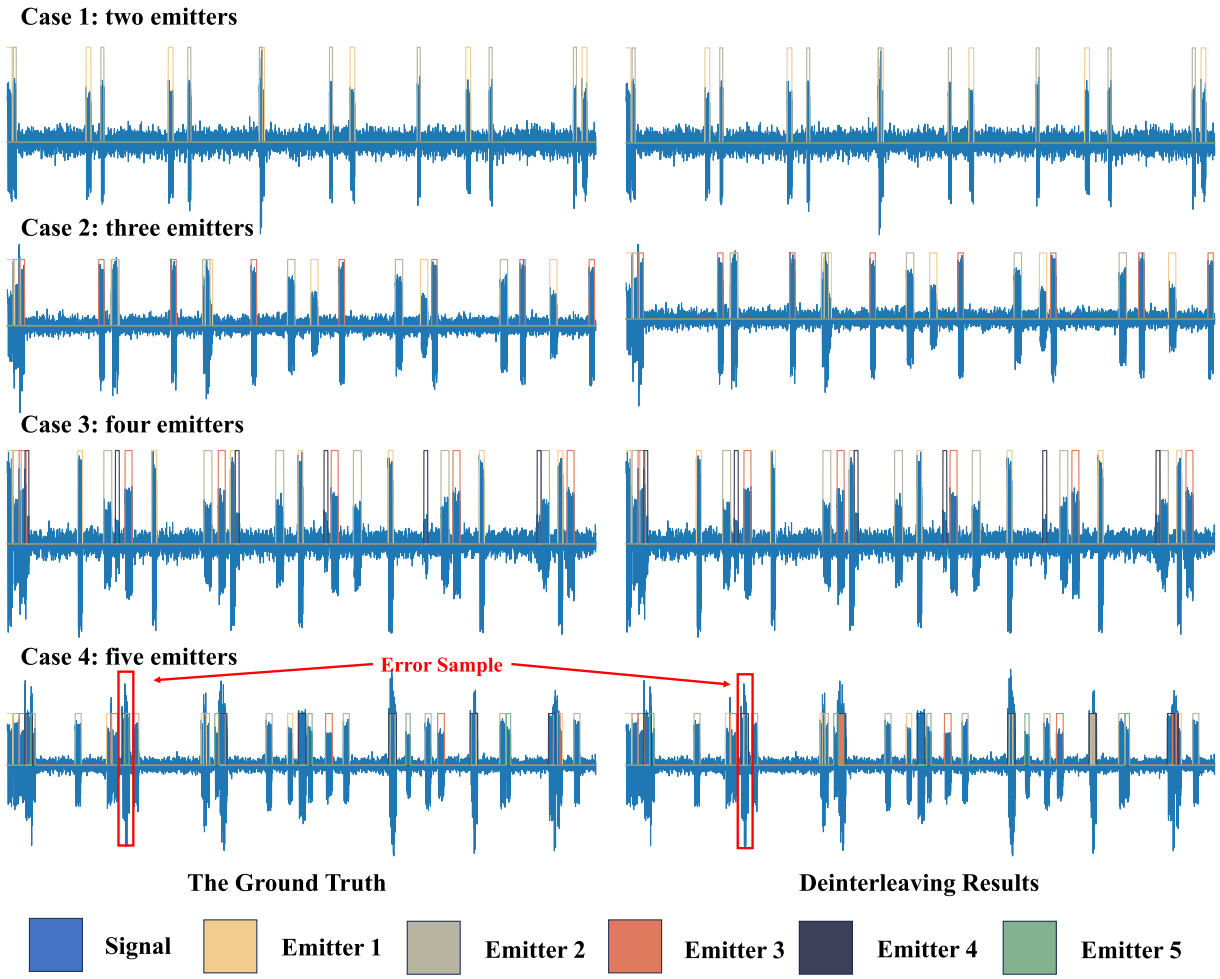

Fig. 4. Comparison results of deinterleaving for different number of radar emitters.

fixed signal bandwidth of 2 MHz, with a Signal-To-Noise Ratio (SNR) set at 20 dB. The dataset consists of 8800 samples, encompassing diverse radar emitter configurations, where each time-domain sample lasts 20 ms. Subsequently, the entire dataset is randomly divided into training and test sets at a ratio of 10:1. Our proposed framework is implemented using the publicly available PyTorch library on an NVIDIA A100 80 GB PCIe GPU.

B. Performance Metrics

In this experiment, the Similarity Coefficient (SIM), Pixel Accuracy (Acc), and Intersection Over Union (IOU) are chosen as quantitative measures to evaluate the performance of our method in the deinterleaving of received signals. The evaluation metrics can be expressed as follows:

$$SIM = \xi(\hat{y}, y) = \frac{\left|\sum_{l=1}^{L}\sum_{n=1}^{N} \hat{y}_{l,n} \cdot y_{l,n}\right|}{\sqrt{\sum_{n=1}^{N}\left[\sum_{l=1}^{L} \hat{y}_{l,n}^2 \cdot \sum_{l=1}^{L} y_{l,n}^2\right]}} \tag{11}$$

$$Acc = \frac{TP + TN}{N \cdot L} \tag{12}$$

$$IOU = \frac{TP}{TP + FP + FN} \tag{13}$$

where TP is the true predicted points when the pulse appears, TN is the true predicted points when the pulse does not appears, FP is the false predicted points when the pulse does not appear, and FN is the false predicted points when the pulse appears.

C. Results

In this section, the received signals, comprising different numbers of radar transmitters, undergo processing using the proposed method. A subset of the results is illustrated in Fig.4. Furthermore, to assess the deinterleaving performance of the received signals, the predicted outcomes are compared with the actual labels, and the result is summarized in Table II. As thenumber of radar emitters increases, the number of pulses in the received signal increases significantly and the signal becomes more complex, resulting in a slight degradation of the model's deinterleaving performance.

Besides, we conducted a comparative analysis of the separation performance between the proposed method and the model structures presented in [10], [15], [16], and [17] for the deinterleaving task. As indicated in Table III, compared with most existing refined networks, our method achieves improved deinterleaving accuracy with a marginal increase in complexity.

TABLE II
DEINTERLEAVING PERFORMANCE WITH DIFFERENT NUMBERS OF RADAR EMITTERS

	2	3	4	5
SIM	0.994	0.963	0.956	0.903
Acc	0.999	0.996	0.993	0.982
IOU	0.987	0.920	0.890	0.781

TABLE III
PERFORMANCE COMPARISON

	DCN	U-Net	U2Net	SSD	**CAU-Net**
SIM	0.603	0.658	0.637	0.763	**0.932**
Acc	0.955	0.974	0.963	0.950	**0.991**
IOU	<0.5	<0.5	<0.5	0.501	**0.831**
Parameters	**0.61M**	2.71M	14.7M	1.17M	2.76M
FLOPs	4867.0M	**2755.1M**	9223.9M	9446.4M	2756.7M

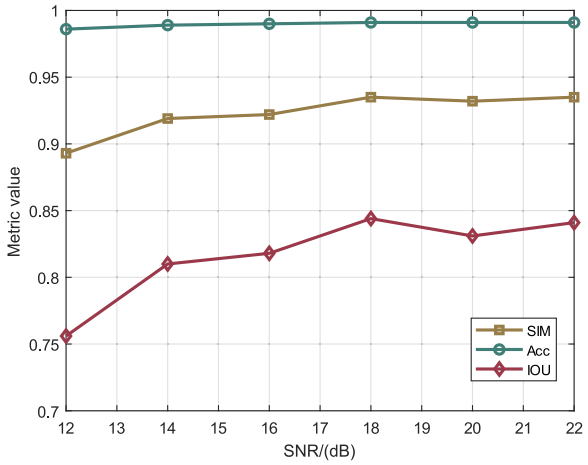

Fig. 5. The curves of the deinterleaving performance under different SNR conditions.

Moreover, we evaluated the performance of the proposed method under various Signal-to-Noise Ratio (SNR) conditions, with the results illustrated in Fig. 5. The performance remains stable when handling datasets with differing SNR levels.

V. CONCLUSION

To summarize, the deinterleaving method devised utilizes a CAU-Net architecture that employs the original received signal, departing from the traditional PDWs-based approach. The method dynamically adapts to deinterleaving by learning received signals from varying numbers of radar emitters. Moreover, a convolutional attention module is integrated during encoding to augment the model's feature learning capabilities. Experimental results substantiate the model's efficacy, showcasing consistent high-performance separation, even when dealing with complex modulation modes employed by each radar emitter.

REFERENCES

[1] S. Saperstein and J. Campbell, "Signal recognition in a complex radar environment," *Electron*, vol. 3, no. 1, p. 8, Mar. 1977.
[2] H. K. Mardia, "New techniques for the deinterleaving of repetitive sequences," *IEE Proc. F Radar Signal Process.*, vol. 136, no. 4, p. 149, 1989.
[3] D. Milojević and B. Popović, "Improved algorithm for the deinterleaving of radar pulses," *IEE Proc. F Radar Signal Process.*, vol. 139, no. 1, p. 98, 1992.
[4] D. Nelson, "Special purpose correlation functions for improved signal detection and parameter estimation," in *Proc. IEEE Int. Conf. Acoust. Speech Signal Process.*, vol. 4, 1993, pp. 73–76.
[5] Y. Liu and Q. Zhang, "An improved algorithm for PRI modulation recognition," in *Proc. IEEE Int. Conf. Signal Process., Commun. Comput. (ICSPCC)*, Oct. 2017, pp. 1–5.
[6] X. Li, Z. Huang, F. Wang, X. Wang, and T. Liu, "Toward convolutional neural networks on pulse repetition interval modulation recognition," *IEEE Commun. Lett.*, vol. 22, no. 11, pp. 2286–2289, Nov. 2018.
[7] Z.-M. Liu and P. S. Yu, "Classification, denoising, and deinterleaving of pulse streams with recurrent neural networks," *IEEE Trans. Aerosp. Electron. Syst.*, vol. 55, no. 4, pp. 1624–1639, Aug. 2019.
[8] Z.-M. Liu, "Pulse deinterleaving for multifunction radars with hierarchical deep neural networks," *IEEE Trans. Aerosp. Electron. Syst.*, vol. 57, no. 6, pp. 3585–3599, Dec. 2021.
[9] X. Li, Z. Liu, Z. Huang, and W. Liu, "Radar emitter classification with attention-based multi-RNNs," *IEEE Commun. Lett.*, vol. 24, no. 9, pp. 2000–2004, Sep. 2020.
[10] W. Chao, S. Liting, L. Zhangmeng, and H. Zhitao, "A radar signal deinterleaving method based on semantic segmentation with neural network," *IEEE Trans. Signal Process.*, vol. 70, pp. 5806–5821, 2022.
[11] P. Sun et al., "Boosting signal modulation few-shot learning with pre-transformation," in *Proc. IEEE Int. Conf. Acoust., Speech Signal Process. (ICASSP)*, 2023, pp. 1–5.
[12] S. Wei, Q. Qu, Y. Wu, M. Wang, and J. Shi, "PRI modulation recognition based on squeeze-and-excitation networks," *IEEE Commun. Lett.*, vol. 24, no. 5, pp. 1047–1051, May 2020.
[13] Z. Yu, J. Tang, and Z. Wang, "GCPS: A CNN performance evaluation criterion for radar signal intrapulse modulation recognition," *IEEE Commun. Lett.*, vol. 25, no. 7, pp. 2290–2294, Jul. 2021.
[14] Q. Lv, Y. Quan, W. Feng, M. Sha, S. Dong, and M. Xing, "Radar deception jamming recognition based on weighted ensemble CNN with transfer learning," *IEEE Trans. Geosci. Remote Sens.*, vol. 60, 2022, Art. no. 5107511.
[15] O. Ronneberger, P. Fischer, and T. Brox, "U-net: Convolutional networks for biomedical image segmentation," *Proc. 18th Int. Conf.*, Munich, Germany, Oct. 2015, pp. 234–241.
[16] K. He, X. Zhang, S. Ren, and J. Sun, "Deep residual learning for image recognition," in *Proc. IEEE Conf. Comput. Vis. pattern Recognit.*, 2016, pp. 770–778.
[17] X. Qin, Z. Zhang, C. Huang, M. Dehghan, O. R. Zaiane, and M. Jagersand, "U2-net: Going deeper with nested U-structure for salient object detection," *Pattern Recognit.*, vol. 106, Oct. 2020, Art. no. 107404.